THE USE OF MONTE CARLO SIMULATIONS FOR THE INTERPRETATION OF LIGHT SCATTERING AND FLUORESCENCE DATA ON SELF-ASSEMBLING POLYMER SYSTEMS IN SOLUTIONS

Pavel MATĚJÍČEK[1], Filip UHLÍK[2], Zuzana LIMPOUCHOVÁ[3] and Karel PROCHÁZKA[4,*]

Department of Physical and Macromolecular Chemistry, Faculty of Science, Charles University, Albertov 6, 128 43 Prague 2, Czech Republic; e-mail: [1] matej@vivien.natur.cuni.cz, [2] uhlik@natur.cuni.cz, [3] zl@vivien.natur.cuni.cz, [4] prochaz@vivien.natur.cuni.cz

Received December 14, 2007
Accepted February 5, 2008
Published online March 17, 2008

Dedicated to Professor William R. Smith on the occasion of his 65th birthday.

In this feature article, we demonstrate the usefulness of tailor-made computer simulations for the interpretation of experimental data. Two examples of studies on self-assembling copolymer systems (by light scattering and fluorescence spectroscopy) performed some time ago are reviewed. It is shown how some unexpected and confusing results could have been interpreted using of Monte Carlo simulations. In both cases, a short outline of the experimental study including the motivation and the most important results is given first. Then the results of simulations are described and discussed with respect to the questions generated by experimental work. In this paper, we included both unpublished and already published data. Thus, the interpretation of the behavior and general conclusions are formulated in a retrospective way. The paper shows that simulations based on a considerably simplified model can complete the mosaic of evidences necessary for a reasonable interpretation of experimental results and can help to understand basic principles of their behavior. The necessary condition is that the model, even though strongly simplified, has to show all essential qualitative features of the behavior.

Keywords: Polymer self-assembly; Polyelectrolyte micelles; Polyelectrolyte brushes; Charged osmotic brush; Monte Carlo simulations; Poisson–Boltzmann equation; Light scattering; Fluorescence; Nonradiative energy transfer.

Collect. Czech. Chem. Commun. 2008, Vol. 73, No. 3, pp. 293–313

doi:10.1135/cccc20080293

Motto: "Everything should be as simple as possible, but not simpler."

Albert Einstein

High-molar-mass block copolymers containing a long hydrophobic block, such as polystyrene and a long polyelectrolyte block, e.g., poly(methacrylic acid) or a neutral water-soluble block, such as poly(ethylene oxide) are insoluble in aqueous media. The self-assembled multimolecular micelles can be prepared indirectly, e.g., by stepwise dialysis from 1,4-dioxane-rich aqueous mixtures against water-rich mixtures and finally against aqueous buffers[1]. The resulting micelles are usually fairly monodisperse spherical nanoparticles containing compact cores formed by insoluble blocks and shells formed by soluble polyelectrolyte blocks. As water is an extremely strong precipitant for polystyrene, the cores are kinetically frozen. It means that the exchange of unimers between micelles ceases and micelles do not dissociate upon dilution.

Polymeric micelles offer a number of applications. They have been studied by many research groups, e.g., as vehicles in targeted drug delivery[2]. In our laboratory, we have been studying the behavior of self-assembling and self-organizing block copolymers by a number of experimental techniques, such as static and dynamic light scattering, steady-state and time-resolved fluorescence techniques, size exclusion chromatography, electrophoretic methods, etc.[3] In the last decade, we also investigated the surface-deposited polymer nanoparticles by atomic force microscopy[4]. In our studies, we always tried to combine different experimental techniques in order to minimize the danger of misinterpretation. Nevertheless, the behavior of micelles is complex and experimental techniques used in our laboratory are indirect (fluorescence) or model-dependent (scattering techniques). Therefore, an independent insight into the studied problem at the molecular level is needed. Independent pieces of information completing the mosaic of evidences and allowing for an unambiguous explanation of the observed behavior can be obtained by computer simulations. Based on our experience, a well-designed computer simulation, based on a sound, even though simplified model, can serve as a benchmark helping to formulate correct interpretation of experimental data[5].

In this feature article, we offer two illustrative examples of already published studies of polymer systems. To make the paper as comprehensive as possible, we focus on Monte Carlo (MC) technique only, even though we have been using also molecular dynamics and self-consistent field calcula-

tions for the interpretation of our experimental results. We would like to point out that we reserve a privilege to interpret the data in a bit retrospective way, i.e., from the perspective of the up-to-date level of knowledge. The paper is organized as follows. In the next part, we describe the model of micelles and the MC simulation technique. Further we give two examples of performed studies. We always outline experimental study first and than we discuss the results of simulations and formulate general conclusions based on the combined study.

THEORETICAL MODEL USED FOR MONTE CARLO SIMULATIONS

We use MC simulation[6] on a simple cubic lattice and study the shell behavior of a single micelle only. Because we model the behavior of shells of kinetically frozen micelles, we emulate a spherical polymer brush, tethered to the surface of a hydrophobic spherical core. The association number is taken from experiment. The size of the core, lattice constant (the size of the "lattice Kuhn segment") and the effective number of lattice segments are recalculated from experimental values on the basis of the coarse graining parametrization[7].

The segment–segment and segment–solvent interactions are described by contact interactions between nearest beads (or free lattice sites – in case of the solvent). We use the most common matrix of interaction parameters in which the "reference interactions", i.e., those where solvent is involved, are zero. The used parameters are: $\varepsilon_{S-S} = 0$, $\varepsilon_{PMA-S} = 0$, $\varepsilon_{C-S} = 0$, $\varepsilon_{PMA-PMA} = -0.27$, $\varepsilon_{PMA-C} = 0.8$ ($\varepsilon_{C-C} = 0.8$), where S, C and PMA stand for solvent (empty lattice site, occupied implicitly by solvent), C core (lattice point at the surface of the core) and the PMA bead (the Kuhn lattice segment, irrespectively of ionization).

The electrostatic interactions (effective in aqueous solutions of annealed polyelectrolytes) are treated indirectly by solving the spherically symmetrical Poisson–Boltzmann equation (PBE) for the electrostatic potential[8] $\phi(r)$

$$\frac{1}{r^2}\frac{\mathrm{d}}{\mathrm{d}r}\left(r^2\frac{\mathrm{d}\phi}{\mathrm{d}r}\right) = -\frac{\rho}{\varepsilon_0\varepsilon_r} \qquad (1)$$

where ε_0 and ε_r are the vacuum permittivity and the relative (position-dependent) permittivity of the dielectric medium, respectively. The charge density $\rho(r)$ includes both the charge of the micelle and of all small ions

$$\rho = \sum_i q_e z_i [x_i] c_0 N_A \qquad (2)$$

where q_e is the elementary charge, z_i the charge number, $[x_i]$ are the relative concentrations of individual charged species, c_0 = 1 mol/l is the standard concentration and N_A is the Avogadro constant.

We consider the following components in the system: COOH, COO^-, H_3O^+, OH^-, Na^+ and Cl^-. Not all of them are independent since they have to fulfill the following relations

$$K_w = a_{H_3O^+} a_{OH^-} \quad \text{and} \quad K_A = \frac{a_{H_3O^+} a_{COO^-}}{a_{COOH}} \tag{3}$$

where K_w and K_A are the ion product of water and the effective dissociation constant describing the dissociation of carboxylic groups in PMA, respectively. The activities of components a_i are calculated using the Debye–Hückel limiting law[8]. The effective dissociation constant for poly(methacrylic acid) in solutions as a function of ionic strength and degree of ionization was measured by Morcellet et al.[9] and by Porasso et al.[10]. Nevertheless, we use the constant value pK_A 4.69 for monomeric methacrylic acid as a rough, although reasonable first approximation[11], because most theoretical calculations for polyelectrolytes employ pK_A for the monomeric units.

The only independent parameters used in our simulations are: pH and ionic strength $I = \sum \frac{1}{2}[x_i] z_i^2$. The position-dependent concentrations of small ions are expressed according to the Boltzmann theorem as follows

$$[x_i(r)] = [x_i]_\infty \exp\left[\frac{-q_e z_i \phi(r)}{kT}\right]. \tag{4}$$

When the position-dependent concentration of H_3O^+ is substituted in the definition of the dissociation constant K_A (Eq. (3)), using $[COO^-]$ = η-[COOH], where η is the position-dependent concentration of PMA segments, which we obtain by MC simulation, we get

$$[COO^-(r)] = \frac{\eta}{1 + [H_3O^+(r)]_\infty \exp[-q_e \phi(r)/kT] \gamma_+ \gamma_- / K_A} \tag{5}$$

where γ_+ and γ_- are the Debye–Hückel activity coefficients of H_3O^+ and COO^-, respectively. This formula together with the Metropolis criterion[6d] (in which both the short-range and long-range electrostatic interactions are combined) actually bridges the indirect treatment of electrostatic forces with the mechanistic MC simulation and provides the self-consistent solu-

tion of the problem. Finally, we may write the following expression for the position-dependent charge density

$$\rho(r)/q_e c_0 N_A = I_\infty (e^{-q_e\phi/kT} - e^{q_e\phi/kT}) - \\ - \frac{\eta}{1+[H_3O^+(r)]_\infty \exp[-q_e\phi(r)/kT]\gamma_+\gamma_-/K_A} \quad (6)$$

which can be inserted in the right-hand-side of Eq. (*1*). Then the differential equation (*1*) is solved numerically (for details, see ref.[7]) and the electrostatic potential $\phi(r)$ is used for the calculation of the contribution of electrostatic potential energy in the Metropolis acceptance criterion[6d].

In summary, the computer simulation for micelles with shells formed by an annealed polyelectrolyte is a combination of MC with the self-consistent field treatment of electrostatic forces. However, it goes far beyond the mean-field approximation. It is also evident from simulation snapshots (see below) that the a priori assumption of the spherical symmetry of the electrostatic field (which is an inherent feature of studied micelles) does not impose a strong constraint on instantaneous chain conformations.

POLYELECTROLYTE BEHAVIOR AT LOW IONIC STRENGTH AT pH CLOSE TO pK_A

Motivation

The properties of solutions of polyelectrolyte micelles are predetermined by the polyelectrolyte behavior of micellar shells, which can be, in the first approximation, regarded as convex polyelectrolyte brushes. Depending on the degree of charging and ionic strength, the polyelectrolyte brush can undergo several patterns of behavior. In systems where the density of charge on the polyelectrolyte chains is high, the electrostatic force acting on counterions is strong and prevents their escape into bulk solvent. Hence the brush remains electrically neutral. At low ionic strengths, the osmotic pressure is high (mainly due to counterions) and individual brush-forming chains are strongly stretched. The brush is swollen and obeys the osmotic regime. In solutions with high ionic strength, the excess of small ions screens electrostatic interactions and the brush collapses, obeying the salted brush regime.

In quenched polyelectrolytes, the degree of ionization is fixed and depends only on the synthesis. In annealed polyelectrolytes, the degree of

ionization depends on pH and ionic strength making their behavior very rich. Some time ago, we speculated that in annealed polyelectrolyte systems at pH close to pK_A, when the dissociation is strongly suppressed and the density of the fixed charge is low, the attractive electrostatic force is weak and the counterions could escape into bulk solvent because they gain considerable translational entropy. Very soon we came to the conviction that this new regime (at that time, not yet experimentally proven) that we call the "charged osmotic brush regime" deserves to be revealed.

Outline of Experimental Study and the Most Important Observations

Polystyrene-*block*-poly(methacrylic acid), PS-PMA, micelles were prepared by stepwise dialysis of 1,4-dioxane-rich aqueous solutions of a diblock PS-PMA copolymer (weight average molar mass, M_w = 39.6 × 10^3 g/mol, PS mass fraction, w_{PS} = 0.52, polydispersity, M_w/M_n = 1.12) in solvents with increasing content of water and finally in pure water. Micelles were characterized by static (SLS) and dynamic (DLS) light scattering (for experimental details, see ref.[12]). The experimental Zimm plot in a sodium borate buffer, c = 0.05 mol/l, used for evaluation of the mass-average molar mass of micelles, $(M_w)_M$ = 3.8 × 10^6 g/mol and of their radius of gyration, R_G = 20 nm, is shown in Fig. 1.

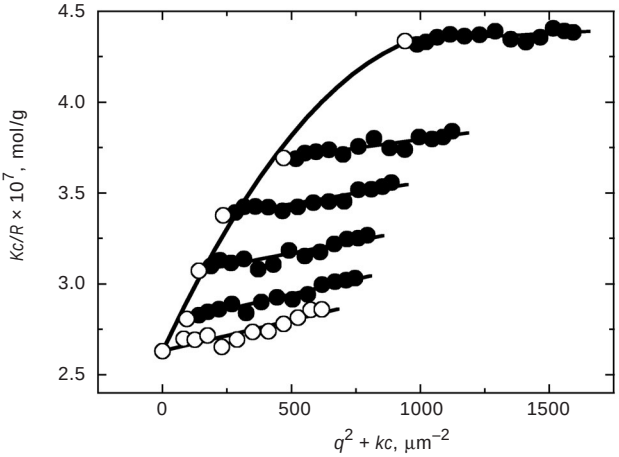

FIG. 1
The Zimm plot for PS-PMA micelles in 0.05 M sodium tetraborate. The values extrapolated to a zero scattering angle and diminishing polymer concentration are marked by hollow points

The plotted quantity $Kc/R(q,c)$ in the Zimm plot for the constant polymer concentration on the squared magnitude of the scattering vector q^2 is almost linear. It indicates that in the region of the used concentrations, monodisperse micelles interact only weakly with each other. Their interaction can be described by the excluded volume effect. This behavior exhibits itself in a polynomial dependence of the quantity $Kc/R(c)$ extrapolated to a zero scattering angle on the micellar concentration. As shown in Fig. 1, not only slightly positive value of the second virial coefficient A_2 contributes when extrapolation to zero polymer concentration is performed, but also virial expansion of higher degrees takes place.

The micelles were further characterized by atomic force microscopy (AFM; for details, see ref.[12]) after their deposition on fresh mica surface. A typical AFM scan of micelles deposited on mica surface (Fig. 2) shows fairly monodisperse spherical nanoparticles.

The Zimm plot of micelles in a solution with extremely low ionic strength, which was prepared by repeated dialysis against an excess of deionized water in plastic flasks (to prevent potential increase in ionic strength due to alkaline metal ions released from glass) is shown in Fig. 3. The concentration region towards both low and high limits is broader than that in Fig. 1. One does not have to be an expert in light scattering to realize an enormous difference between the behavior at low and at medium ionic strength. At relatively low concentrations, the q dependences start to decline from the linear one and later they exhibit minima. Such type of behavior is due to spatial correlations between individual scatterers (micelles). This feature is typical for strongly interacting systems. Occurring at concen-

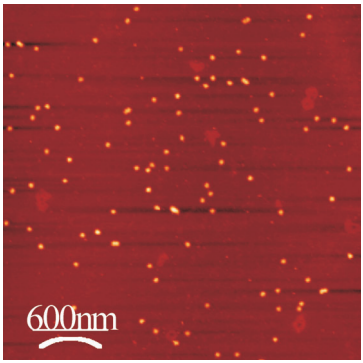

FIG. 2
AFM scan of PS-PMA micelles deposited on mica surface

trations where the average distances between micelles reached up to 5–10 times their diameter, the behavior suggests that the long-range electrostatic forces between significantly charged micelles are responsible for structural correlations of scatterers and for the observed destructive interference of the scattered light.

We can conclude that our experimental study indicated that the "charged osmotic brush" regime, in which counterions escape into bulk solvent, can be reached when the experiments are performed carefully. Our study provided the very first indirect evidence of, at that time only hypothetical and by recognized theoreticians highly questioned behavior of polyelectrolyte micelles. We were looking for an independent support and performed a MC study described below.

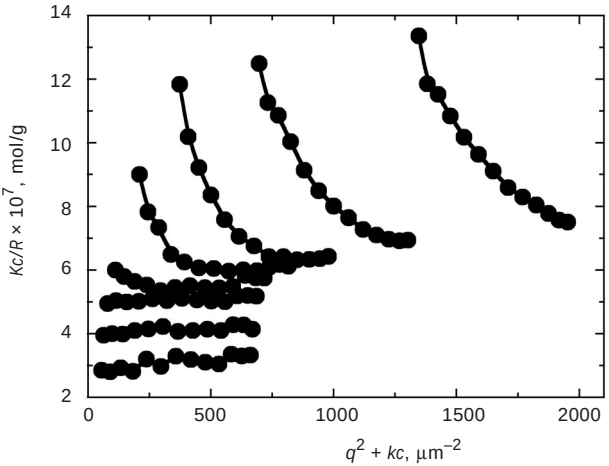

FIG. 3
The Zimm plot for PS-PMA micelles in pure water

Results of Simulations

To get a sufficient insight into the polyelectrolyte behavior of micellar shells necessary for unambiguous interpretation of the above experimental data, we performed a series of coarse-grained lattice MC simulations for PE brushes tethered to spherical cores that mimic the studied micelles as close as possible. Details on the coarse-graining procedure can be found in ref.[7]. MC simulations yield (i) snapshots of micellar structures and (ii) a number of ensemble average characteristics, such as radius of gyration R_G (as a func-

tion of pH and *I*) and its distribution, segment density profiles of the shell-forming blocks, ionization profiles, radial dependences of the electrostatic potential, etc. To give an idea on simulated structures, we show two snapshots that depict typical micelles at different pH (pH 5 and 7, Figs 4 and 5, respectively). A comparison of both snapshots shows increasing swelling of micellar shells with pH due to the well-known effect of ionization. The dependences of gyration radii on pH are shown in Fig. 6. The snapshots and rather trivial dependences of radii of gyration on pH have been included in order to document the basic correctness of the model and

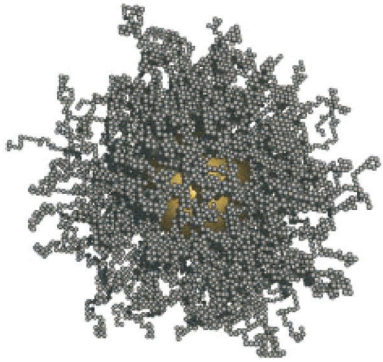

FIG. 4
Typical snapshot of PS-PMA micelles at pH 5

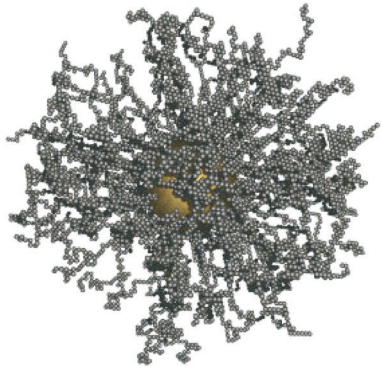

FIG. 5
Typical snapshot of PS-PMA micelles at pH 7

the simulation procedure used. We would like to point out that the pronounced coiling of the shell-forming chains at the micellar periphery, where the degree of dissociation and electrostatic interactions are important, demonstrates that the constraint imposed by the a priori assumed

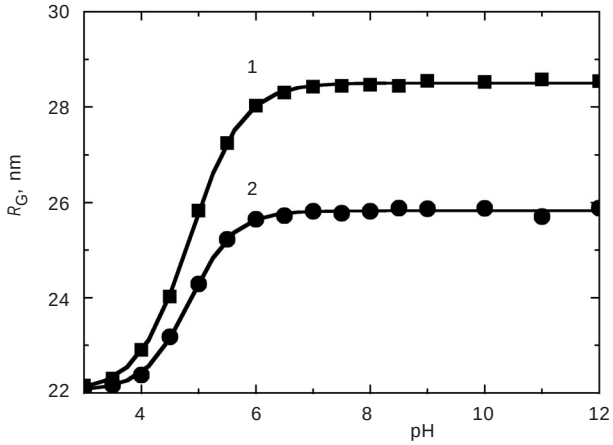

FIG. 6
Simulated dependence of gyration radii, R_G, of PS-PMA micelles on pH for ionic strength 0.01 (1) and 0.1 (2)

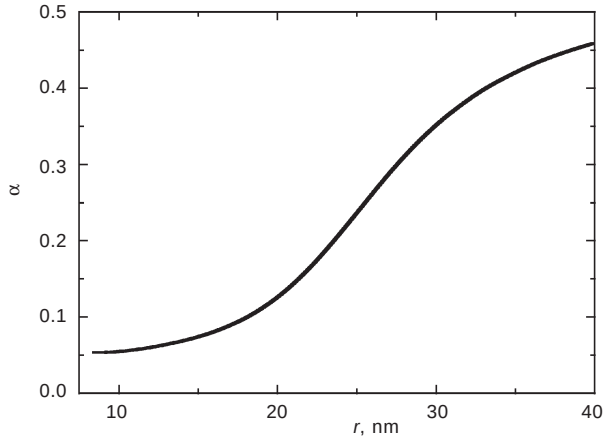

FIG. 7
Simulated dependence of the degree of dissociation of COOH groups in PS-PMA micelles, α, as a function of the distance from the micellar center, r, for pH 5 and ionic strength 0.001

spherical symmetry of the electrostatic field is weak and does not artificially restricts the conformational behavior of individual chains.

Further we discuss data that are directly related to the polyelectrolyte behavior at low I close to pK_A. Figure 7 shows the degree of dissociation of ionizable COOH groups for pH 5 and I = 0.001. Figure 8 shows the electrostatic potential as a function of r (the distance from the micellar center) and the r-dependent concentration profiles of the positive and negative charge for the same condition. It is evident that the electrostatic potential at the periphery of micelles is significantly negative and that there exists an excess of negative charge in the shell and an excess of positive charge around micelles.

In our MC study, we focused on the behavior of infinitely dilute solutions: we simulated a single micelle only. We are fully aware of the fact that at low albeit finite concentrations, the properties and conformations of micelles interacting over long distances can slightly differ from those predicted by our simple model. However, even though we model an infinitely dilute solution and we cannot calculate the micelle–micelle interaction in the cloud of counterions, the results of simulation support the concept of charged osmotic brush.

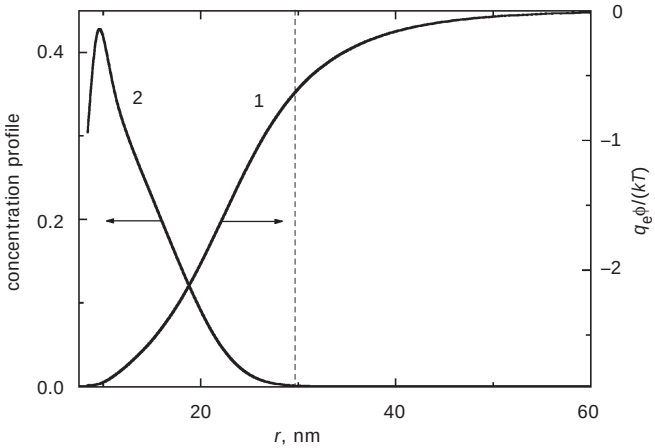

FIG. 8
Simulated concentration profile (2) and electrostatic potential (1) in PS-PMA micelles as a function of the distance from the micellar center, r, for pH 5 and ionic strength 0.001

CONFORMATIONAL BEHAVIOR OF MICELLES WITH HYDROPHOBICALLY MODIFIED SHELL-FORMING BLOCKS

Motivation

Many systems based on water-soluble block copolymer micelles have been developed and studied as vehicles for targeted drug delivery purposes[2]. The copolymers used for such applications have to be biocompatible and biodegradable. Their micelles have to assure the solubilization of considerable amounts of hydrophobic drugs in their hydrophobic cores. They have to contain targeting (recognition) groups at their periphery. An obvious recipe for the incorporation of targeting groups in micelles is their chemical attachment at the ends of water-soluble shell-forming blocks. However, the recognition groups are usually large and of complex chemical structures (e.g., antigens) and not all of them are strongly hydrophilic. They can be amphiphilic or slightly hydrophobic, which means that their interaction with water does not have to be favorable. Therefore, they could try to bury in the shell (which is hydrophilic, but less polar than water) in the effort to escape from the energetically unfavorable environment. If this happened, their avoidance of the uppermost part of the shell would have a very negative impact on the drug delivery efficiency. The outlined worst-case scenario of the failure of a laboriously developed system underlines the importance of experimental studies on well-defined model systems and computer simulations.

We addressed the above problem by studying a system of modified PS-PMA micelles with PMA blocks end-tagged by strongly hydrophobic groups in mixtures of water with 1,4-dioxane (where the dissociation of COOH groups is suppressed) and in purely aqueous media (where electrostatic effects dominate the behavior)[13]. The used copolymer is not biocompatible. However, the micelles are monodisperse and very stable in aqueous media. Therefore they represent a suitable generic system for physicochemical research. We used anthracene (An) as the end-attached hydrophobic group which allowed for fluorescence study. Starting the experimental study, we assumed that the hydrophobic probe would try to optimize the interactions with its microenvironment and would try to "hide" in the shell. However, if anthracene succeeds in returning towards the core and buried in the shell, the PMA block (containing ca. 300 methacrylic acid units) to which anthracene is attached has to collapse or form a loop. It reduces the entropy. Hence we expected a broad distribution

of An distances from hydrophobic micellar cores as a result of an intricate enthalpy-to-entropy interplay.

Outline of Experimental Study and the Most Important Observations

For the experimental study, we used two almost identical PS-PMA samples, very similar to that studied in the previous case. The first one was fluorescence-tagged with one pendant naphthalene group (Np) between the PS and PMA blocks. The second sample was tagged with Np in the same way as the previous one, but also by one An at the end of the PMA block. The two fluorophores, Np and An, were used because they represent a suitable pair for nonradiative energy transfer (NRET) study and they can be relatively simply incorporated (covalently attached) in the studied system[14].

Experimental results were obtained by two experimental techniques – light scattering and time-resolved fluorescence spectroscopy, TRFS. In TRFS, the fluorescent sample is excited with an intense ultrashort excitation pulse and the fluorescence intensity, which decays on the nanosecond timescale, is measured[15]. In the simplest case, the natural fluorescence decay is exponential. As all fluorescence properties are strongly influenced by surrounding molecules, the deviations from the natural decay report on interactions of the fluorophore with its microenvironment.

In the studied micellar system, all attached Np molecules (excitation energy donors) are localized at the core-shell interface. The most important Np fluorescence quenching is expected to be due to nonradiative (dipole–dipole) energy transfer to energy traps (An) that are located up to distances comparable with the Förster radius, R_F (for the Np–An pair ca. 2.1 nm)[16]. The rate of the transfer strongly decreases with the distance r, varying $\sim(R_F/r)^6$ and therefore An at distances larger than R_F do not almost affect the excited Np. As demonstrated in the previous part, the thickness of the shell depends on pH and ionic strength and usually ranges from 15 to 40 nm. Hence it is clear that the Np emission could be affected only by An groups that return deep in the shell. The nonradiative energy transfer study should prove if a fraction of shell-embedded An are located in the close vicinity of the core.

The quenching of the time-resolved Np emission due to the naphthalene-to-anthracene energy transfer is shown in Fig. 9. The NRET-affected fluorescence decays for micelles in three solvents differing in polarity (mixtures of 1,4-dioxane and water with increasing water content) are normalized by the decays in the absence of traps. The broken-like curves obtained in aqueous media, consisting of a steeply decreasing part and a constant

part almost without any curved part in-between, are of interest. They cannot be reasonably well reproduced by assuming any type of a continuous unimodal distribution of Np–An distances[17]. The broken shape suggests the

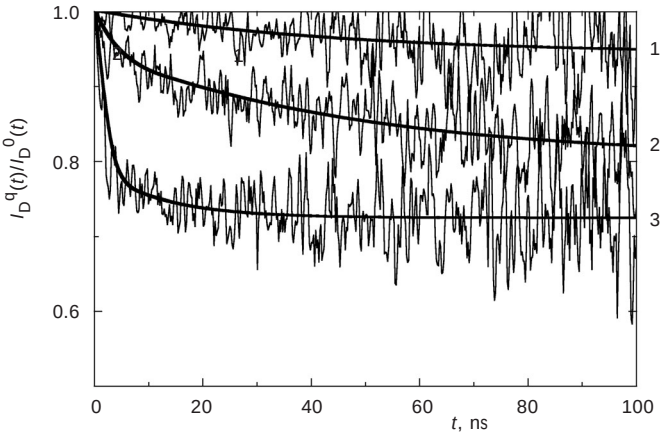

FIG. 9
Experimental kinetic NRET curves, i.e., the time-resolved fluorescence decays of naphthalene emission affected by NRET to anthracene (in PS-PMA micelles containing both Np and An groups) normalized by decays unaffected by NRET (in micelles containing only Np groups) in three different solvents: in 5% water/95% 1,4-dioxane (1), in 20% water/80% 1,4-dioxane (2), and in water (3). Experimental data (noisy) are fitted to smooth multiexponential functions

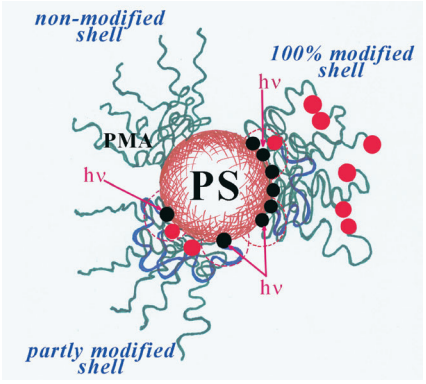

FIG. 10
Schematics of fully hydrophobically modified micellar shell (right-hand-side segment), partly hydrophobically modified micellar shell (lower left-hand-side segment), and unmodified micellar shell (upper left-hand-side segment)

existence of two types of Np donors which are either very strongly affected by NRET, or fully unaffected. In a spherically symmetrical system, in which all Np groups are uniformly distributed in a narrow spherical layer at the core/shell interface, the concept of two types of Np groups looks strange. However, it can be rationalized when we postulate a rather specific conformational behavior of An-tagged shell-forming chains, which is depicted in Fig. 10.

The model assumes the coexistence of two distinctly different conformations created by the same shell-forming chains in each micelle under equilibrium conditions. The coexisting forms are (i) strongly collapsed and (ii) stretched chains. Segment "100% modified shell" in Fig. 10 depicts the described situation. Accepting the above scheme, it is clear that some pendant An traps can strongly affect some Np donors because they return in their immediate vicinity, while other Np donors remain unaffected. Because in a typical fluorescence measurement the fraction of excited fluorophores is less than 10^{-6}, maximally one Np group per micelle is excited (in most cases none). Hence the fluorescence decay from some micelles is unaffected by NRET and that from others is very strongly quenched. The ensemble average normalized time-resolved fluorescence response can look like the curve 3 in Fig. 9 in this particular case.

Results of Simulations

A pronounced bimodal distribution of chain conformations in a micelle that contains ca. 10^2 chains is something that one would hardly expect in an equilibrium system. Even though bimodal distributions were tentatively proposed for some other equilibrium polymer systems earlier[18]. To elucidate the studied problem, we performed a series of simulations for modified micellar shells using the MC technique for neutral systems and the combined MC – mean field simulation technique described in the first part for charged aqueous systems. Figure 11 compares the distributions of radial distances of end segments from the core in the modified and unmodified systems. Figure 12 presents the distribution function of random Np–An pair distances, i.e., the distribution of distances of An traps around a randomly excited Np donor, averaged over all donors in the modified micellar system. This allows for the calculation of fluorescence decays. Both functions are bimodal in the modified system (with a narrow peak in the region of small distances), which confirms our working hypothesis used for the above-outlined tentative interpretation of NRET results. The naphthalene fluores-

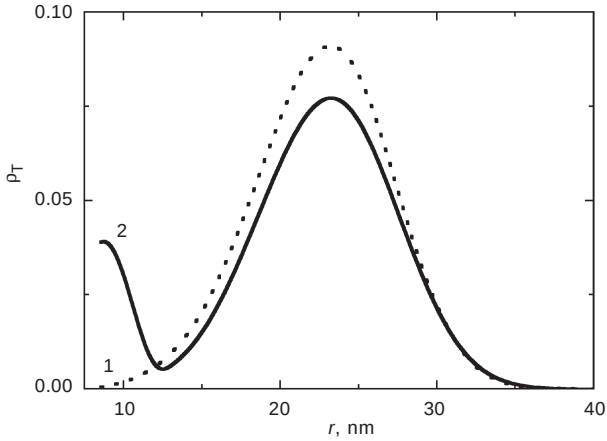

FIG. 11
Simulated distributions of radial distances of end segments from the core in hydrophobically modified (solid curve 2) and unmodified (dotted curve 1) PS-PMA micelles

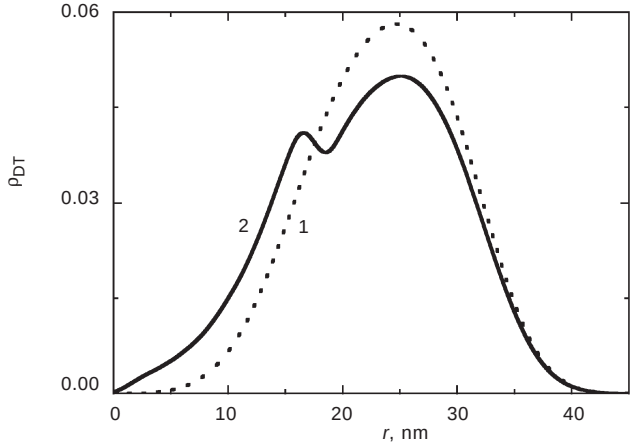

FIG. 12
Simulated distribution functions of Np–An pair distances in hydrophobically modified (solid curve 2) and unmodified (dotted curve 1) PS-PMA micelles

cence decay can be calculated using the $P_{NA}(r_{NA})$ function; however, the MC method offers a more direct evaluation of its shape. The simulation yields a number of independent micelles and for each equilibrated micelle, it is possible to solve numerically the master equation[19] describing the probability $p(t)$ that the excitation is located at time t at the fluorophore that was excited at time $t = 0$

$$\frac{\mathrm{d}p}{\mathrm{d}t} = -\left(\frac{1}{\tau_D} + \sum_{i=1}^{n} k(r_i)\right)p \qquad (7)$$

where τ_D is the natural (unaffected) fluorescence lifetime of the donor (Np) and $k(r_i)$ are the position-dependent rate transfer constants

$$k(r_i) = \left(\frac{1}{\tau_D}\right)\left(\frac{R_F}{r_i}\right)^6 \qquad (8)$$

describing the rate of NRET for individual pairs i formed by the randomly excited Np and all fixed An traps in one micelle. The first term of the right-hand-side of Eq. (*7*) describes the depletion rate of the excited state by fluorescence and the sum of $k(r_i)$ multiplied by p describes the net effect of NRET in the system with a fixed position of all An. The averaging over different arrangements of traps around the excited donor (i.e., over all possible conformations of the shell-forming chains in the micellar system) yields the following formula for the enumeration of the experimentally accessible fluorescence decay

$$I_D^q(t) = I_D^0(t)\left\langle \exp\left(-\sum_{i=1}^{n}\left(\frac{R_F}{r_i}\right)^6\left(\frac{t}{\tau_D}\right)\right)\right\rangle . \qquad (9)$$

The comparison of experimental and calculated decays that is depicted in Fig. 13, shows a good quantitative agreement of both curves.

A more detailed analysis of the conformational behavior of the shell-forming chains can be based on the 2D function (Fig. 14) which depicts the number fractions of chains with particular combinations of their radii of gyration R_G and distances of the end segment from the core, R_T. It shows two well-marked regions where the function attains high values. It shows that R_G and R_T of individual chains are correlated. So far we have assumed that a fraction of chains form either loops or collapsed conformations. The fact that R_G and R_T are simultaneously either small or large means that the

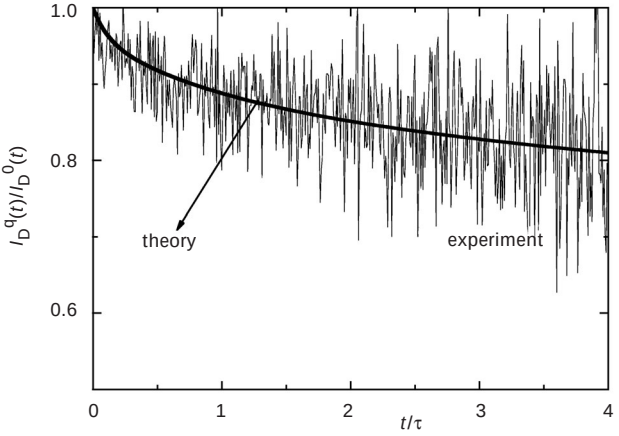

FIG. 13
Comparison of experimental data (noisy), multiexponential fit of experimental data and simulated curve describing the NRET kinetics in modified PS-PMA micelles (the fitted and simulated curves perfectly overlap)

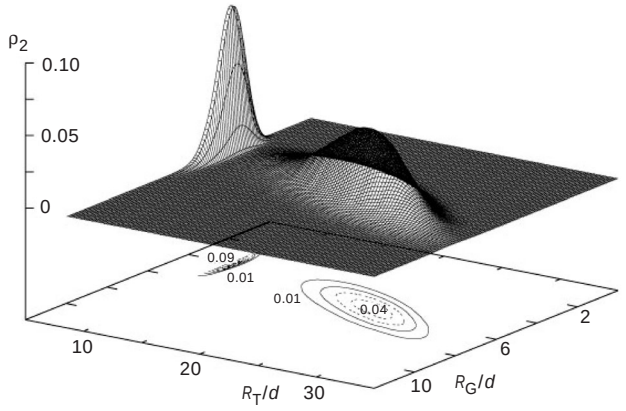

FIG. 14
2D-density function, $\rho_2(R_G,R_T)$, describing the fractions of hydrophobically modified shell-forming chains with given radii of gyration, R_G, and distances of the end-segment from the micellar center, R_T (the radii are divided by a unity length d)

chains with the end-attached An localized close to the core are collapsed and do not form open loops.

To summarize results of MC simulations, we can say that the computer study confirmed our hypothesis on the bimodal distribution of conformations of the modified shell-forming chains. The obtained results are interesting both from the theoretical and practical points of view. As concerns the practical design of micelle-based systems with the end-attached targeting groups, the study indicates that the choice of a suitable group requires great care. In real drug delivery systems, the fraction of end-attached groups is usually low. Therefore we further studied the micelles with mixed shells containing 80% of unmodified and 20% of modified PMA chains by light scattering, fluorescence and computer simulations. Both experimental and computer-based techniques have shown that the unmodified chains adopt stretched conformations, while all chains with end-attached hydrophobic molecules (anthracene) recoil back and come close to the core (see segment "partly modified shell" in Fig. 10). This means that if the used targeting group is not fully hydrophilic, the danger of the delivery efficiency loss cannot be ignored.

CONCLUDING REMARKS

Experimental data on systems, the behavior of which is complex, can be strongly confusing, especially if indirect techniques are used. Many "benchmark" techniques routinely used in polymer research are model-dependent (scattering techniques) or indirect (fluorescence spectroscopy). Fluorescence emission is generally influenced by interactions of the excited fluorophore with surrounding molecules, which means that is prone to a number of parasite effects. This means that either independent data on the behavior or a sound model of the system behavior is necessary. Computer simulations are a powerful tool that offers independent pieces of information necessary to complete the knowledge. However, they offer much more. They provide an unbiased opinion whether the working hypothesis for interpretation of experimental data and the general model of the behavior are basically correct or erroneous.

In this feature article, we presented only two examples of the help provided by computer simulations to experimentalists. In our group, we have been using not only Monte Carlo, but also molecular dynamics and self-consistent field calculations which helped us in a number of experimental studies. It is our conviction that close cooperation between experimental-

ists and theoreticians is necessary because it broadens and accelerates the research.

This work is a part of the research plan of the Faculty of Science of the Charles University (MSM0021620857) supported by the Ministry of Education, Youth and Sports of the Czech Republic. It was further supported by the Grant Agency of the Academy of Sciences of the Czech Republic (Grants IAA400500703 and IAA401110702), by the Grant Agency of the Czech Republic (Grant 203/07/0659) and the Marie Curie Research and Training Network (RTN 505027, Polyamphi). The authors would like to thank the METACentrum (CESNET) for the computer time.

REFERENCES

1. Munk P., Ramireddy C., Tian M., Webber S. E., Procházka K., Tuzar Z.: *Makromol. Chem., Macromol. Symp.* **1992**, *58*, 195.
2. a) Harada A., Kataoka K.: *Prog. Polym. Sci.* **2006**, *31*, 949; b) Zhao Q., Ni P. H.: *Prog. Chem.* **2006**, *18*, 768; c) Rodriguez-Hernandez J., Checot F., Gnanou Y., Lecommandoux S.: *Prog. Polym. Sci.* **2005**, *30*, 691; d) Gil E. S., Hudson S. A.: *Prog. Polym. Sci.* **2004**, *29*, 1173; e) Volodkin D., Mohwald H., Voegel J. C., Ball V.: *J. Controlled Release* **2007**, *117*, 111; f) Michel A., Izquierdo A., Decher G., Voegel J. C., Schaaf P., Ball V.: *Langmuir* **2005**, *21*, 7854.
3. a) Štěpánek M., Procházka K.: *Langmuir* **1999**, *15*, 8800; b) Štěpánek M., Procházka K., Brown W.: *Langmuir* **2000**, *16*, 2502; c) Štěpánek M., Podhájecká K., Tesařová E., Procházka K., Tuzar Z., Brown W.: *Langmuir* **2001**, *17*, 4240; d) Humpolíčková J., Procházka K., Hof M., Tuzar Z., Špírková M.: *Langmuir* **2003**, *19*, 4111.
4. a) Matějíček P., Štěpánek M., Uchman M., Procházka K., Špírková M.: *Collect. Czech. Chem. Commun.* **2006**, *71*, 723; b) Matějíček P., Uchman M., Lokajová J., Štěpánek M., Procházka K., Špírková M.: *J. Phys. Chem. B* **2007**, *111*, 8394.
5. a) Havránková J., Limpouchová Z., Štěpánek M., Procházka K.: *Macromol. Theory Simulations* **2007**, *16*, 386; b) Jelínek K., Limpouchová Z., Uhlík F., Procházka K.: *Macromolecules* **2007**, *40*, 7656.
6. a) Siepman J. I., Frenkel D.: *Mol. Phys.* **1992**, *75*, 59; b) Rosenbluth M. N., Rosenbluth A. W.: *J. Chem. Phys.* **1955**, *23*, 356; c) Limpouchová Z., Procházka K.: *Macromol. Theory Simulations* **2004**, *13*, 328; d) Metropolis N., Rosenbluth M. N., Rosenbluth A. W., Teller H.: *J. Chem. Phys.* **1953**, *21*, 1087.
7. Uhlík F., Limpouchová Z., Jelínek K., Procházka K.: *J. Chem. Phys.* **2004**, *121*, 2367.
8. Hounter R. J.: *Foundation of Colloid Science*, Vol. 1, p. 331. Oxford Science Publications, Oxford 1995.
9. Morcellet M., Wozniak M.: *Macromolecules* **1991**, *24*, 745.
10. Porasso R. D., Benegas J. C., van der Hoop M. A. G. T.: *J. Phys. Chem. B* **1999**, *103*, 2361.
11. Lide D. R., Frederikse H. P. R. (Eds): *Handbook of Chemistry and Physics*, 76th ed. CRC Press, Boca Raton 1995.
12. Matějíček P., Podhájecká K., Humpolíčková J., Uhlík F., Jelínek K., Limpouchová Z., Procházka K., Špírková M.: *Macromolecules* **2004**, *37*, 10141.
13. a) Matějíček P., Uhlík F., Limpouchová Z., Procházka K., Tuzar Z., Webber S. E.: *Macromolecules* **2002**, *35*, 9487; b) Matějíček P., Humpolíčková J., Procházka K., Tuzar Z., Špírková M., Hof M., Webber S. E.: *J. Phys. Chem. B* **2003**, *107*, 8232; c) Matějíček P.,

Uhlík F., Limpouchová Z., Procházka K., Tuzar Z., Webber S. E.: *Collect. Czech. Chem. Commun.* **2002**, *67*, 531.
14. a) Schillen K., Anghel D. F., Miguel M. G., Lindman B.: *Langmuir* **2000**, *16*, 10528; b) Martin T. J., Webber S. E.: *Macromolecules* **1995**, *28*, 8845; c) Holden D. A., Guillet J. E.: *Macromolecules* **1980**, *13*, 289.
15. Lakowicz J. R.: *Principles of Fluorescence Spectroscopy*. Plenum Press, New York and London 1983.
16. Berlman I. B.: *Energy Transfer Parameters of Aromatic Compounds*. Academic Press, New York and London 1973.
17. a) Uhlík F., Limpouchová Z., Matějíček P., Procházka K., Tuzar Z., Webber S. E.: *Macromolecules* **2002**, *35*, 9497; b) Uhlík F., Limpouchová Z., Jelinek K., Procházka K.: *J. Chem. Phys.* **2003**, *118*, 11258.
18. Shusharina N. P., Linse P.: *Eur. Phys. J. E* **2001**, *4*, 399.
19. Wieb Van Der Meer B., Coker G., Simon Chen S. Z.: *Resonance Energy Transfer. Theory and Data*. Wiley-VCH, New York, Chichester, Weinheim, Brisbane, Singapore, Toronto 1991.